Beyond Coulomb: Stochastic Friction Models for Practical Grasping and Manipulation

Zixi Liu, *Graduate Student Member, IEEE,* and Robert D. Howe, *Fellow, IEEE*

Abstract—Reliable grasping and manipulation in daily tasks and unstructured environments require accurate contact modeling and grasp stability estimation. A key component is the coefficient of friction, which is variable and dependent on many factors. However, robotics applications often use Coulomb's model of friction, which ignores this variability and instead assumes that the coefficient of friction is a constant. In this work, we conducted sliding experiments with robot fingers and a robot hand, and show that rubber friction varies strongly with normal force F_n and contact velocity v, and includes a significant stochastic component. We present a framework for modeling the coefficient of friction μ as a distribution rather than a constant, and show how this distribution can be narrowed when given a prior on F_n or v. For a given distribution, the likelihood of slipping is a continuous function with respect to the tangential-to-normal force ratio, instead of a step function according to Coulomb's law. By modeling friction as a function of F_n and v, we demonstrate that friction parameters can be estimated using regression models from a single sliding stroke of the fingertip against the object surface, and that strokes spanning a larger range of F_n-v space provide better friction estimates. These results can be applied to grasp control to enable a quantitative trade-off between the likelihood of slipping vs. grasp force levels, and to sliding manipulation planning by elucidating the relationship between desired velocity and anticipated force levels. Application of this model to machine learning has the potential to enhance reinforcement learning and sim-to-real transfer by providing more accurate representations of frictional behavior.

Index Terms—Friction, Friction Variability, Contact Modeling, Grasping, Dexterous Manipulation, In-Hand Manipulation, Uncertainties in Grasping and Manipulation

I. INTRODUCTION

FRICTION between fingers and objects plays a critical role in reliable grasping and manipulation. The exceptional dexterity of the human hand in performing a wide range of grasping and manipulation tasks is dependent on our ability to sense contact properties, particularly friction properties, using thousands of mechanoreceptors located in the fingertips [1]. This superb tactile sensing capability allows us to perform tasks that are challenging for robots, such as recognizing when something is about to slip out of hand or controlling finger motions to reorient an object within the hand. Understanding friction is essential for executing controlled sliding and avoiding accidental drops.

Zixi Liu is with the School of Engineering and Applied Sciences, Harvard University, 150 Western Ave., Boston, MA 02134 USA (e-mail: zixiliu@g.harvard.edu).

Robert D. Howe is with the School of Engineering and Applied Sciences, Harvard University, 150 Western Ave., Boston, MA 02134 USA, and also with RightHand Robotics Inc., 237 Washington St., Somerville, MA 02143 USA (e-mail: howe@seas.harvard.edu).
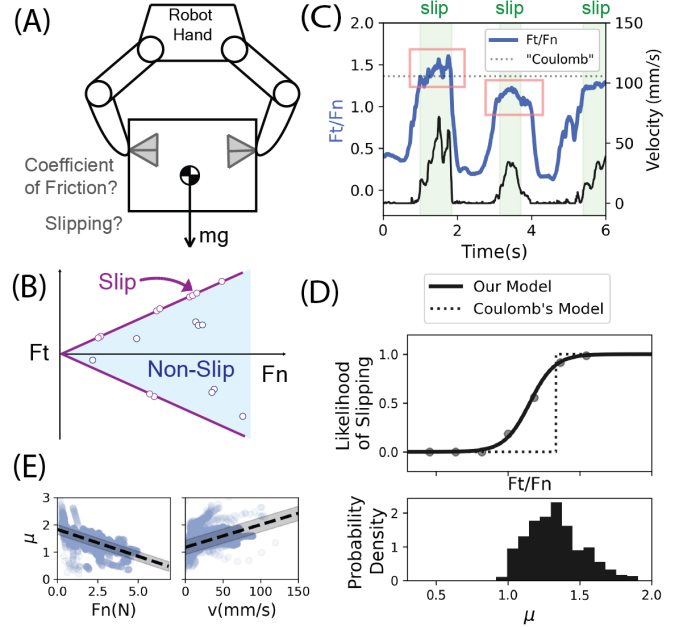
Fig. 1. (A) A typical robot-object interaction via friction. (B) A 2-D illustration of a friction cone in Coulomb's model. (C) An example of F_t/F_n variation as an elastomeric fingertip starts and stops sliding. The F_t/F_n ratio varies extensively even within a single slip episode, and peak values change significantly between episodes. (D) Fingertip sliding data shows that instead of a constant $\mu_{Coulomb}$ at which slipping occurs, the coefficient of friction, μ, is a stochastic variable with probability density function shown in the bottom plot. Using μ to determine slip in this model reports a likelihood of slip instead of a binary slip/no-slip estimate. (E) Measurements of μ as a function of normal force F_n and velocity v, respectively, with mean $\pm$ standard deviation values in black dashed line and adjacent grey shading.

In robotics, Coulomb's law of friction is the cornerstone of both simulation and real-time control (e.g. [2]–[4]). This "law," which is reasonably accurate for many rigid materials, states that the friction or tangential force F_t between two objects is proportional to the normal force F_n pressing them together, or $F_t = \mu F_n$, where μ is the coefficient of friction, which is assumed to be constant for a given fingertip-object material pair (Fig. 1B) [5].

Soft polymeric materials, however, are typically used to cover robot fingers to allow the fingertip to conform to object surfaces and to provide high friction. For these materials, friction is stochastic and variable at the macroscopic level (Fig. 1D). This behavior has been studied extensively in other fields, particularly automotive tires, but has not been applied to robotics. "Quantitative physical analysis began with the observation that the classic Coulombic laws obeyed consistently at rigid body interfaces fail at the interface between a rigid solid and a rubber." [6] This behavior is due to numerous factors. First, soft materials like robot fingertips sliding against rigid surfaces exhibit stick-slip phenomena due to deformation and

detachment waves [6], [7]. In addition, in real-world settings, rubber friction changes due to variations across the object and robot fingers in surface roughness and imperfections, local contamination (dust, liquids, etc.), temperature and humidity level, etc. [6]–[10].

Rubber friction also varies with loading and sliding speed (Fig. 1E), as shown in numerous studies. Important examples include Schallamach's investigation of the relationship between μ, load, and contact area; this resulted in the formulation $\mu = cW^{-1/3}$ where c is a constant and W is the load [11], which is proposed as an alternative to Thirion's formulation $1/\mu = a + bW$, where a and b are constants [12]. Schallamach also showed the dependency of μ on contact velocity [13]. Albertini et al. investigated the stochastic properties of friction [14]. Kang at el. demonstrated the stochastic variability of friction for general mechanical systems [15].

Characterization of friction for robotic control of grasping and manipulation has been a specialized sub-field. Bicchi et al. evaluated μ during the transition from static to dynamic friction in rotational and translational motion [16]. While the data in this paper appear to show stochastic variation in the F_t/F_n ratio, the coefficient of friction is treated as Coulombic, with only static and dynamic values. Cutkosky et al. evaluated multiple materials for robot skin and proposed $\mu = F_n/\tau A$ where τ is the shear strength of the bonded areas and A is contact area [17]. Han et al. also evaluated the relationship between μ and F_n, and proposed $\mu = \tau_0/(F_n/A) + \alpha_0$ where τ_0, α_0 are constants [18]. Zhou et al. modeled the stochastic friction distribution in planar pushing by sampling contact force from appropriate distributions [19]. Ma et al. argued that variability in planar friction is explainable but inevitable in practice, and introduced an anisotropic friction model where friction in x and y directions was individually considered [20]. None of these studies proposed a stochastic model for robot fingertip friction.

In this work, we investigate the variability of the coefficient of friction, μ, as a function of the normal force F_n and contact velocity v, including a random component. Our contributions are four-fold. First, we propose a framework for characterizing μ as a distribution rather than a single constant. We model μ as a stochastic function with respect to F_n and v, and validate this model via experimental data. This implies that the likelihood of slipping under specified loading conditions is a continuous function with respect to the tangential-to-normal force ratio, instead of a step function according to Coulomb's law. Second, the distribution of μ becomes narrower when priors such as a known range of F_n are available. Third, by modeling $\mu = f(F_n, v)$, we can estimate the friction parameters of the function f using a regression model, and demonstrate that these parameters can be reliably estimated with a single stroke by spanning the anticipated F_n-v space of interest. And lastly, the friction model enables quantitative planning of sliding manipulation to answer questions such as: What is an appropriate tangential force if a specific sliding velocity is desired? What contact velocity is likely if a certain contact force is applied? We emphasize that the proposed model is a framework for incorporating the variability of friction into robot planning and control applications, and is not meant to
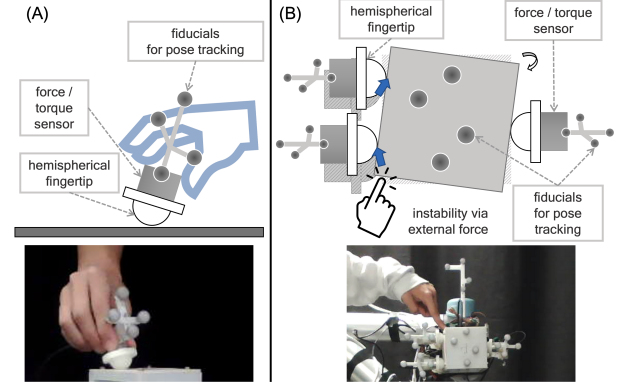

Fig. 2. (A) Handheld experiment: a human operator holds a robot finger and slides across surfaces in varying contact force, velocity, and contact location. (B) Robot hand experiment: the robot hand grasps an object and a human operator applies external force to cause instability, leading to slips on one or more fingertip(s) without pushing the object out of the hand.

be an optimal friction model or an exhaustive investigation of friction parameters across many materials.

The following sections of this paper provide a description of the experimental setup used for data acquisition, an explanation of the theoretical construct, and experimental validation of the four contributions. The paper concludes with a discussion of the implications of our proposed friction modeling framework for robotic control, its integration with machine learning, and its limitations.

II. MEASUREMENT OF FRICTION CHARACTERISTIC

We conducted two sets of experiments: one with a handheld robot finger ("Handheld experiment," Fig. 2A), and another with a three-fingered articulated robot hand ("Robot hand experiment," Fig. 2B).

A. Hardware

Each robot fingers is equipped with a high-precision force/torque sensor (ATI Nano17. Resolution: 1/160 N, 1/32 N·mm, 500 Hz). A hemispherical fingertip is mounted on the force/torque sensor. It consists of a 17-mm-diameter rigid inner layer (Stratasys Vero White) and a 3-mm-thick silicone rubber outer layer (Smooth-On Dragon Skin 30). The robot hand experiment uses a modified tendon-driven three-fingered robot hand (Reflex Hand, RightHand Robotics) with custom-designed fingers with two pin joints and fingertips as described above. A high-precision optical tracking system (Atracsys Fusion Track 500, Resolution: 0.090 mm RMS, 330 Hz) measures the pose of each fingertip and the grasped object using fiducial markers. For the object, we 3D-printed an 80 mm cube (polylactic acid) with fiducials for precise pose tracking. Mounting sites on the sides of the cube mate with plates of various surface materials.

We fabricated side attachment plates in four materials: paint primer (Rust-Oleum 260510 Automotive 2-in-1 Filler & Sandable Primer), smooth paper (cast acrylic sheet surface protection paper), heavyweight paper (heavyweight art paper for dry and wet media), and canvas. Each side attachment has a base layer of laser-cutting acrylic. Then the base layer was coated by spray painting paint primer or gluing paper and

canvas with spray adhesive (Scotch Super 77 Multipurpose Adhesive Spray), flattened with a vinyl squeegee.

B. Data Processing

Data from the force/torque sensors and optical tracking sensor are logged in Robot Operating System (ROS) and synchronized at 300 Hz post-processing. Contact location, contact surface normal, and contact force in the object frame are calculated based on the geometries and poses (from optical tracking) of the robot finger and the object. Since the fingertip is hemispherical, the contact location is found by the normal projection of the center of the hemisphere onto the object's side surface. Contact forces are measured directly on the fingertip via the force/torque sensor.

Contact velocity is defined as the velocity of the contact point on the surface of the object (from optical tracking), with the velocity of the contact point on the fingertip surface (from Intrinsic Sensing [21]) subtracted to compensate for rolling. Velocities are median-filtered with a kernel size of 80 ms.

C. Handheld Experiment

A robot finger is dismounted from the robot hand, and a human operator holds the robot finger and slides it on a flat surface, as shown in Fig. 2A. The human operator executes repeated sliding motions of the fingertip along the flat surface with varying levels of force, velocity, and robot fingertip contact location, leading to diverse sliding profiles. Between strokes, the robot finger comes to a complete stop, and can be lifted from the surface. Here we provided visual feedback to each subject on normal force via real-time plotting, demonstrated how slow (~ 15 mm/s) vs. fast (~ 80 mm/s) stroke looks like, and instructed each subject to cover $0 - 5N$ and slow to fast span while varying fingertip contact locations. We collected 2 minutes $\times$ 4 materials each, across 3 subjects, approximately 27% of which is slipping. For every slip, the contact velocity goes up and down; for slip episodes whose peak velocity is above 10 mm/s, we label the peak and any neighboring samples with a velocity value above 5 mm/s as "slip". This avoids spurious labels due to noise in velocity estimates but captures all significant sliding episodes. For consistency, samples with normal force ≥ 5N or velocities ≥ 150 mm/s are removed. Note that whether a human or a robot executes the experiment will not impact the results, as long as the range of variability is well-covered by confirming coverage post-processing.

D. Robot Hand Experiment

In the robot hand experiment, the robot hand grasps a cubical object with three fingers while a human operator gently and repeatedly applies a varying external force anywhere on the cube, causing it to slip within the grasp of the robot hand without dropping (Fig. 2B). Two trials are collected, each lasting approximately one minute. Samples are labeled slipping when the peak contact velocity is above 5 mm/s.

III. FRICTION MODELS AND ESTIMATION METHODS

A. The Coefficient of Friction is a Stochastic Function

For the remainder of this paper, we define the coefficient of friction as $\mu = F_t/F_n$ when slip is occurring, which can vary
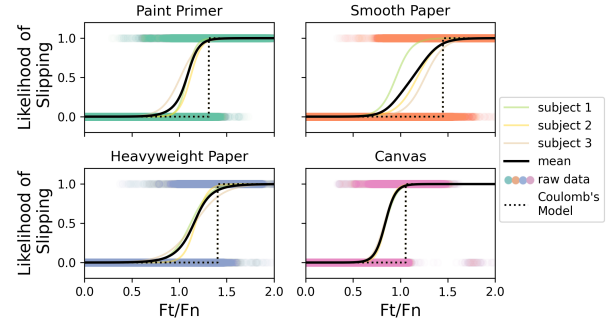

Fig. 3. The likelihood of slip as a function of F_t/F_n across four materials in the handheld experiment. Note that they all observe a range of uncertainty with width differing across materials.

with loading and velocity and include a stochastic component. We contrast this definition of μ to the fixed coefficient of friction assumed by Coulomb's model, which we will refer to as "Coulomb's coefficient of friction", or $\mu_{Coulomb}$.

Fig. 1C shows a typical example from the handheld experiment that illustrates that the coefficient of friction can vary significantly. $\mu_{Coulomb}$ is plotted as a dotted line for reference. While Coulomb's coefficient of friction, commonly sourced from literature databases, is frequently utilized in robotics, its accuracy is often limited with polymeric materials due to the high variability of friction. In this plot, we define $\mu_{Coulomb}$ as the mean value of μ across all data points collected from the same surface material.

Fig. 1E plots the coefficient of friction against normal force and velocity from the same experiments on a single material. These findings confirm their correlation with μ, in agreement with prior studies in the rubber friction literature.

Typically the use of Coulomb's law to determine slip entails comparing the force ratio F_t/F_n to the constant Coulomb's Coefficient of Friction, $\mu_{Coulomb}$, to get a binary prediction: when $F_t/F_n < \mu_{Coulomb}$ the contact will not slip, and when $F_t/F_n \geq \mu_{Coulomb}$ it will. However, these experiments show that in practice, slipping may or may not occur as F_t/F_n approaches $\mu_{Coulomb}$ from either direction, rather than $\mu_{Coulomb}$ behaving as a discrete sharp boundary. Given that the coefficient of friction is variable and stochastic in nature, here we present a framework to estimate the coefficient of friction and its uncertainty.

When F_t/F_n is low compared to $\mu_{Coulomb}$, the likelihood of slipping is 0% in practice; similarly, when F_t/F_n is high, the likelihood of slipping is essentially 100%. Between the two extremes, the likelihood of slip increases as F_t/F_n increases. Fig. 1D shows the probability density of μ across various contact conditions for a single material, which spans the wide range from 1 to 2, as well as the likelihood of slipping, L, as a function of F_t/F_n. L is calculated by binning samples by F_t/F_n and calculating the slip-to-non-slip sample ratio in the perspective bins. We model L by fitting a sigmoid curve to the results. For this material, the model suggests that when $F_t/F_n \leq 0.89$ it never slips, and when $F_t/F_n \geq 1.55$ it always slips. Between these two values, whether a sample point is slipping is uncertain based on F_t/F_n alone but exhibits a probability distribution with defined uncertainty bounds.

Fig. 3 shows the likelihood of slip as a function of F_t/F_n for

the four materials in the handheld experiment across subjects. While there is a difference in the mean value of μ for these diverse materials, as shown by the step function representing Coulomb's model, the plot also shows that in all four cases, the range of uncertainty is substantial and exhibits variation in width as well as its position relative to $\mu_{Coulomb}$ in each case. Note that the widest span, in the case of smooth paper, covers the range from 0.55 to 1.76, indicating that the variability in μ can cover a notable three-fold span. Across subjects, the differences are minimal. Note that for smooth paper, subject 1 applied less variation in their strokes compared to the other subjects (Fig. 9). The significance of this particular detail underscores the fact that covering the desired span of variability is key for repeatability. For the remainder of the analysis, we group the data from all three subjects.

B. Limiting Normal Force or Velocity Range Narrows the Distribution of μ

As expected for rubber friction, the coefficient of friction is correlated with the normal force and contact velocity (Fig. 4). As a result, the distribution of μ becomes narrower when given prior information on normal force and/or contact velocity.
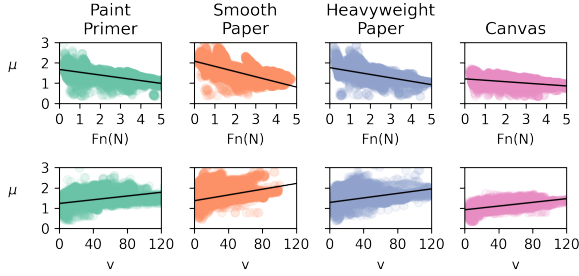

Fig. 4. The coefficient of friction with respect to the normal force (top row) and contact velocity (bottom row) across four materials. Solid line represents linear regression on the data.
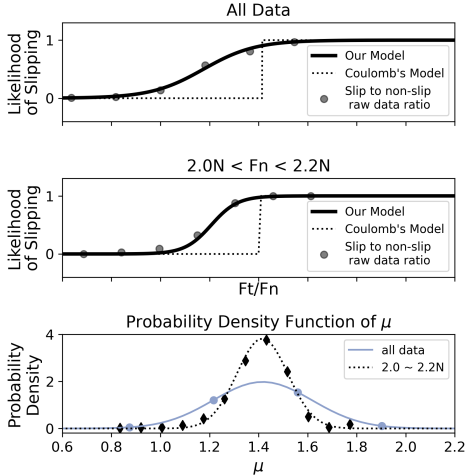

Fig. 5. An example of using prior information on F_n to narrow the distribution of μ. The top plot shows the likelihood of slip (raw data for the slip-to-non-slip ratio of points in a certain F_t/F_n range) vs. F_t/F_n for all data for the heavyweight paper. The middle plot shows the ratio for the force range $2.0N < F_n < 2.2N$. The bottom plot shows the probability density function of μ in the above plots.

Fig. 5 shows an example of all heavyweight paper data vs. data from a limited range of normal force, $2.0N < F_n <$
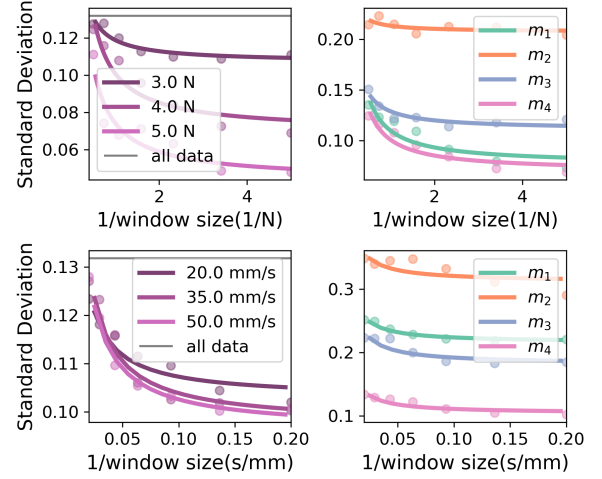

Fig. 6. The distribution width (standard deviation) of μ as a function of the window size of F_n and v. The left column shows variation for different choices of window center value, and the right column shows variation for the four materials (m_1 to m_4 for paint primer, smooth paper, heavyweight paper, and canvas, respectively), centered at $4\ N$ and $20\ mm/s$.

$2.2N$. From the probability density function, we see that with prior information on F_n, the distribution of μ has a smaller standard deviation (0.19 reduces to 0.09). This allows a more precise estimation of the likelihood of slipping. Note that when contact velocity $v > 0$, the contact is by definition slipping, so while limiting the range of velocities will similarly narrow the μ distribution, it will not narrow the likelihood function because the results will be 100% slip for any velocity window.

To demonstrate the effect of window size on distribution width for μ, we show that the shorter the window size, the narrower the distribution becomes, i.e. the lower the standard deviation (Fig. 6).

These findings indicate that the more information available about the instantaneous contact conditions, the narrower the distribution of μ becomes. This also suggests that it may be possible to increase the precision of the model in situations where other factors affecting μ (e.g., temperature or humidity) can be measured.

C. Estimating Friction Parameters Using Regression Models

The observed variability of the coefficient of friction implies that estimation of frictional properties is required for each surface material. A straightforward and useful (although not necessarily optimal) approach is to use linear regression on data generated by a "test stroke" of the robot finger against the material surface.

1) Linear Regression Model: The coefficient of friction μ can be modeled with the linear regression

$$\mu(t) = \beta_0 + \beta_1 v(t) + \beta_2 F_n(t) + \epsilon \qquad (1)$$

where $\beta_0, \beta_1, \beta_2$ are constants specific to a given material, ϵ is a random variable that represents the stochastic variation in μ for this material, and t is time.

We fit the handheld dataset to a linear regression model, resulting in moderately good linear fits and strong statistical significance (Table I). We define the absolute error as $e(t) = |\mu(t) - \hat{\mu}(t)|$ where $\hat{\mu}(t)$ is the estimated $\mu(t)$ from
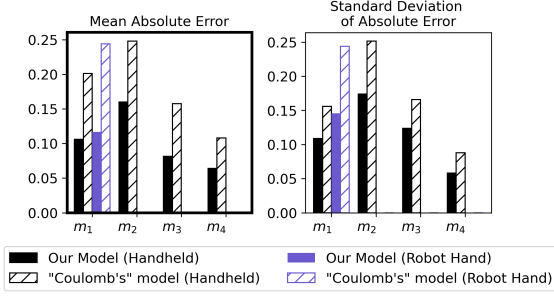
Fig. 7. The mean and standard deviation of absolute error of the estimation of the coefficient of friction for our linear regression model vs. Coulomb's model. Our model outperforms Coulomb's model in all four materials (m_1 to m_4 for paint primer, smooth paper, heavyweight paper, and canvas, respectively). The results from the robot hand experiment are on par with those of the handheld experiment.

the regression model. We approximate the distribution of ϵ by the distribution of e, i.e. $\hat{\sigma}_\epsilon = \sigma_e$. Note that by definition, the mean value of ϵ is 0.

Fig. 7 shows the mean absolute error $\bar{e}$ and the standard deviation of the absolute error σ_e across materials. For comparison, we calculated Coulomb's coefficient of friction $\mu_{Coulomb}$ as the mean value of μ. The results demonstrate that the linear regression model predicts μ more accurately, with $\bar{e}$ and σ_e roughly half the values for Coulomb's model. This suggests that while approximately half the variability of μ for these particular materials is due to random variation, the remaining half is due to dependence on normal force and velocity, which can be compensated for in the linear regression model. We note that here $\mu_{Coulomb}$ is optimized for the dataset and will likely outperform generic Coulomb constants taken from the literature.

We validated this result in a robotic grasping scenario using two trials from the robot hand experiment. First, we fit a linear regression model to one trial (training set); then we evaluate the resulting model on the other trial (test set). The mean and standard deviation of the absolute error for the test set are shown in Fig. 7 next to the handheld dataset results for comparison. Again, the linear regression model significantly outperforms Coulomb's model, and the resulting $\bar{e}$ and σ_e are on par with the results from the handheld dataset, suggesting that the results from the handheld dataset are generalizable to grasping and manipulation scenarios.

When using F_t/F_n to predict slip, the distribution of ϵ from the regression model also sets the bounds of uncertainty. Here we omit v and use the simple linear regression model $\mu = \beta_0 + \beta_2 F_n + \epsilon$, because knowing v would imply knowledge of slip. This can be used to predict the likelihood of slipping, L, from F_t/F_n, with the likelihood function estimated from all the data collected on this material as in Fig. 3.

However, since we know that the coefficient of friction is a function of F_n, we can get a better estimate of the likelihood of slipping if we take F_n into account, i.e. $L = f(F_n, F_t/F_n)$.

TABLE I

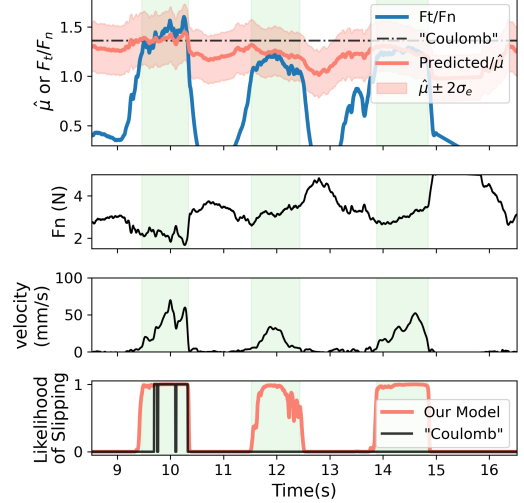| Material	R^2	F	p
Paint Primer	0.643	28500	< 0.0001
Smooth Paper	0.553	17190	< 0.0001
Heavyweight Paper	0.580	25090	< 0.0001
Canvas	0.615	42250	< 0.0001

Fig. 8. An example of the variation in F_t/F_n during and across slipping episodes and the likelihood of slip estimated by our model vs. Coulomb's model. Green highlights denote slipping intervals. Note that our model predicts $\hat{\mu}$ with low error and reports a continuous likelihood of slipping.

First, we fit a likelihood function in small windows of F_n as described in Section III-B. Specifically, for every 0.2 N within the range of F_n between 0.6-4.4 N, we select a 0.6-N-wide window and fit a sigmoid likelihood function defined as $L = 1/(1+e^{-c1(F_t/F_n-c_2)})$. Then we interpolate the estimated parameters as a function of F_n, i.e. $c_1 = f_1(F_n), c_2 = f_2(F_n)$, yielding the general form:

$$L = f(F_n, F_t/F_n) = 1/(1 + e^{-f_1(F_n)(F_t/F_n-f_2(F_n))}) \quad (2)$$

To illustrate the benefits of this approach, we show its performance when applied to the handheld experiment data previously shown in Fig. 1C. As seen in the bottom plot of Fig. 8, Coulomb's model results in a small error during the first slip, but a significant, large error during the second. The predicted coefficient of friction from the regression model, $\hat{\mu}(t)$, however, results in a significantly smaller error during both slips. Here we plot the uncertainty bound $\hat{\mu}(t) \pm 2\sigma_e$ in shaded red, and show that during the second slip where we observe a small error between $\mu(t)$ and $\hat{\mu}(t)$, $\mu(t)$ lies in the region of uncertainty as predicted by our model, and has a high likelihood of slipping. For determining the likelihood of slipping, Coulomb's model detects parts of the first slip and completely misses the second slip with a binary 0/100% estimation, while our model reports a significant, if not 100% likelihood of slipping during all slips. As expected, as $F_n(t)$ decreases, $\hat{\mu}(t)$ increases, and as $F_n(t)$ increases, $\hat{\mu}(t)$ decreases, resulting in a more accurate prediction.

2) Estimating Friction Parameters with a Single Stroke: One advantage of using a linear regression model is the relatively small number of parameters that must be estimated, i.e. $\hat{\beta}_0, \hat{\beta}_1, \hat{\beta}_2$, and $\hat{\sigma}_\epsilon$. This means that when encountering a new material with unknown frictional properties, the robot can simply perform stroke(s) on its surface in order to acquire a reasonable estimate of these model parameters.

A key issue is the reliability of the parameter estimates for small samples, e.g. a single stroke. The precision of the regression coefficients $\hat{\beta}_i$ can be calculated in terms of their estimated standard errors, which are functions of the
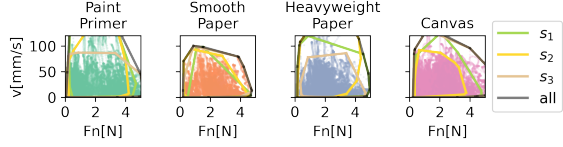
Fig. 9. The F_n-v span of all the data collected in the handheld experiment.
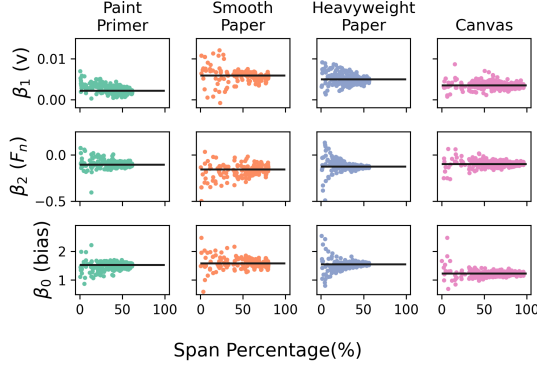

Fig. 10. Variability in the estimation of the friction parameters, $\beta_0, \beta_1, \beta_2$ from $\mu = \beta_0 + \beta_1 v + \beta_2 F_n + \epsilon$ with respect to varying F_n-v span percentage.

covariance matrix of the regression coefficients and $\hat{\sigma_\epsilon}$ [22]. Values are typically provided by multiple regression software. In general, estimates of the friction parameters with a small dataset such as a single stroke have the best precision when the collected samples cover a large range of the independent variables, and include the range that is likely to be encountered in the planned task scenario. Specifically, since we model μ as a function of F_n and v, the stroke should cover the anticipated span of F_n-v.

To evaluate the effects of limiting the span in the F_n-v space of data collection, we calculate the variability in friction parameter estimation from small samples that do not cover the entire range. For this analysis, we define 100% span percentage as covering the entire F_n-v span of the full handheld experiment dataset (Fig. 9). Specifically, we find the convex hull of the slipping samples spanning the F_n-v space and calculate its area A_{full}. For the ith subset of samples, we find the corresponding convex hull area A_i and define the span percentage as $A_i/A_{full} \times 100\%$.

We randomly select n (not necessarily consecutive) strokes from the handheld dataset, calculate the span percentage, and estimate the friction parameters $\hat{\beta}_0, \hat{\beta}_1, \hat{\beta}_2$ from (1). Here n is an integer randomly sampled 500 times from the range 1~40. We found that friction parameters estimated from datasets spanning a small percentage of the F_n-v space are highly variable, and as the datasets cover a higher percentage of span, the variability is reduced and the parameters converge to steady state (Fig. 10). While the rate of convergence varies across materials, in most cases the variability reaches close to a steady state above 50% span.

In our analysis, we used varying numbers of strokes, but the key is the percentage of the F_n-v span instead of the number of strokes. Therefore, it is possible that a single stroke covering $\geq 50\%$ span can reliably estimate the friction parameters $\beta_0, \beta_1, \beta_2$. To perform such a stroke, it is important to monitor the span coverage during the data collection process. More strokes can be added as needed, and more data would mean a more accurate estimation of the distribution of ϵ.

D. Stochastic Friction Model for Practical Control

In addition to slip prediction and estimation of the coefficient of friction, the friction model described in Section III-C can be used for practical control, specifically controlled sliding and anticipation of sliding speed in contact motion planning.

1) Controlled Sliding: In some applications such as controlling object re-orientation within the hand via sliding, it is important to control the contact velocity or target a specific speed. Using this model, one can find the ideal tangential force F_t to apply to the contact to achieve a desired contact velocity v_d. By fitting data to the general form in (1), we can estimate the friction parameters, $\hat{\beta}_0, \hat{\beta}_1, \hat{\beta}_2$, and use them to find the estimated coefficient of friction, $\hat{\mu}$. This can be re-arranged to solve for the target tangential force to be applied, F_t^{target}:

$$\hat{\mu} = \left.\frac{F_t}{F_n}\right|_{slip} = \hat{\beta}_0 + \hat{\beta}_1 v + \hat{\beta}_2 F_n$$
$$F_t^{target} = \hat{\beta}_0 F_n + \hat{\beta}_1 v_d F_n + \hat{\beta}_2 F_n^2 \tag{3}$$

For F_n, one option is to apply a suitable F_n via force control, then plug in v_d to find the optimal tangential force F_t^{target} to apply to the contact; alternatively, the applied F_n can be measured and F_t adjusted to F_t^{target} to reach the desired contact velocity.

2) Prediction of Contact Velocity for Motion Planning: In other applications, it could be helpful to predict contact velocity given measurements of F_n and F_t in grasp control or manipulation. This can be helpful for adapting to the current contact condition, planning subsequent motions, and perceiving how fast and how far the robot finger has traveled when contact velocity cannot be measured. For instance, if friction parameters can be estimated using benchtop sensors in a constrained environment such as the laboratory, this model can be deployed outside the lab to predict velocity if the slipping condition is known. Similar to the derivation of (3) above, using this model we can plug in the measurements F_n, F_t and find the estimated velocity, $\hat{v}$ as

$$\hat{v} = \left(\left.\frac{F_t}{F_n}\right|_{slip} - \hat{\beta}_0 - \hat{\beta}_2 F_n\right)/\hat{\beta}_1 \tag{4}$$

IV. DISCUSSION & CONCLUSION

A holistic understanding of friction properties is key for reliable and effective grasping and manipulation. The above results demonstrate that for elastomeric robot fingertips, modeling the coefficient of friction as a single constant as in Coulomb's law of friction results in large errors. This work presents a framework for analyzing and understanding friction in robotic applications. We model friction as a stochastic variable that is a function of normal force F_n and contact velocity v, whose distribution can be narrowed when given a prior on F_n and/or v. This model predicts the likelihood of slipping as a continuous function with respect to F_t/F_n, instead of a step function according to Coulomb's law. Friction parameters can be estimated using regression models with as little as a single stroke, and can be applied for practical control of grasping and manipulation.

We emphasize that the contribution of this study is not an optimal friction model nor an exhaustive evaluation of all
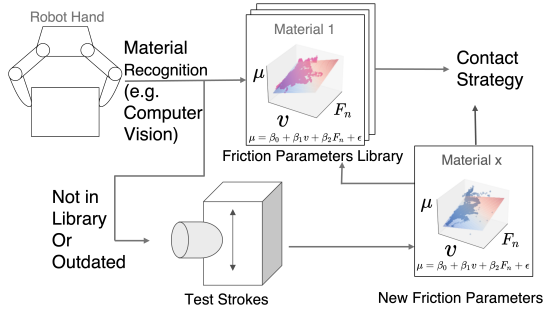
Fig. 11. An illustration of the proposed workflow where a library of friction parameters is created to streamline the process of finding friction parameters. When a material is not found in the library, the robot can proceed to perform test strokes to acquire friction parameters for this material, add it to the library, then apply it to contact perception and planning.

materials in all conditions, rather, the provision of a framework and method for incorporating more accurate friction models in robotic applications. However, specifics of this approach, particularly the variation of μ with F_n and v, have been confirmed by the rubber friction literature to be generalizable across a wide range of materials and conditions.

We became aware of the limits to the prediction of robot friction in grasping during our attempts to develop controllers that accurately predict the onset of slip. Despite the use of state-of-the-art sensors and painstaking refinement of experimental methods, we found slip prediction had limited accuracy, even in the simplest grasping configurations. This led to the investigation of rubber friction models, and the creation of the framework proposed here that accounts for the inherent variability of polymer friction.

A. Implications for Robot Control

Treating the coefficient of friction, μ, as a random variable enables reasoned trade-offs in grasp force for planning and task control. For example, if a particular task requires confidence in stability at the $\leq 0.1\%$ risk of dropping an object (e.g. manipulating a full cup of coffee), then knowledge of the friction distribution function prescribes using a low value for μ, at the price of higher grasp forces thus increased risk of damaging the object. On the other hand, if only 5% stability is needed (e.g. picking up a shirt), then the distribution function prescribes using a higher μ for planning and control, resulting in lower grasp forces.

While the test stroke(s) should center on the range of F_n and v to be used in the manipulation task, spanning wider ranges and collecting more samples allow more precise estimates of friction model parameters and better estimates of ϵ. For tasks where fine control is required, extended data collection might be worth the time and labor to collect and process.

This framework enables the workflow illustrated in Fig. 11: a library of friction parameters for a collection of materials can be generated with offline data in a laboratory setting. When a robot is about to grasp an object, a material-recognition mechanism (e.g. friction sensors, computer vision algorithm, etc.) can determine what material it is and retrieve its corresponding friction parameters. These friction parameters can then be applied to contact strategy. This is particularly useful when either F_n or v is not available from in-hand sensing. The robot will still be able to use the results, albeit in a limited

fashion. In the event that a material is not found in the library, the robot can proceed to perform a test stroke to acquire the friction parameters for this material, add them to the library, then apply them to contact perception and planning.

Local slip sensing could minimize or eliminate the need for friction models for detecting slipping. However, such sensors are an active area of research (e.g. [23]–[26]) and there is no widely adopted practical solution as of yet. Another way to detect slip is to adopt a slip detection algorithm using signals from various in-hand sensors. This is also an active area of research [27]–[31], for which our method provides a practical solution. However, slip sensing alone cannot anticipate slipping before it occurs. For many applications, detecting a slip once it has already occurred may be too late to be useful, in which case the likelihood of slipping can provide valuable insight.

B. Implications for Machine Learning

1) Simulation and Transfer Learning: State-of-the-art physics engines for simulating contact for robot grasping and manipulation often struggle to fully and accurately represent the complex behavior at contacts. When the coefficient of friction is represented in simulation, Coulomb's law of friction is often assumed, and $\mu_{Coulomb}$ is often arbitrarily set to 1, taken from the literature, or user-defined.

In this work, we show that the coefficient of friction is a stochastic variable that changes significantly with respect to normal force and velocity. The maximum observed value of μ can be as large as three times the minimum, spanning a wide range. This implies that it is important to include this function in simulations. An accurate representation will not only make simulations more realistic but in the case of sim-to-real adaptation via transfer learning, may also result in faster and better learning.

2) Reduced Sensor Suite in Deployment Using Reinforcement Learning: In our prior work, we introduced an approach to reliable grasping using Reinforcement Learning (RL). In this approach an RL controller is trained using contact-sensor-based reward functions, but with minimal contact information in the state feedback. After training, the system was capable of reliable grasping, even with minimal contact sensing on the deployed version of the hand [32]. Analogously, we propose training an RL model on a robot hand equipped with high-precision tactile sensing for contact force, contact velocity, and slip condition. This information can be used in the reward function to achieve high accuracy in estimating μ and/or detecting slips, but omitted from the state feedback. This model can then be deployed on robot hands with a reduced sensor suite, lowering their cost and streamlining the fabrication process. Further studies will be required to validate the effectiveness of this proposed strategy.

C. Limitations and Considerations

1) Linear Regression vs. More Sophisticated Models: Although our analysis focused on linear regression models, this method is not constrained to this particular model. In fact, a more sophisticated model for $\mu = f(F_n, v, ...)$ could further improve the results. For μ as a function of F_n, we implemented

the linear model as well as the following models based on the references in Section I: $\mu = aF_n + b$, $\mu = 1/(aF_n + b)$, and $\mu = a/F_n^3 + b$. We show the corresponding R^2 values in Table II. For μ as a function of v, analytical models were not available from the literature to the best of our knowledge. Ultimately, we adopted the linear regression model based on its simplicity, transparency, interpretability, and the fact that it is on par with other proposed analytical models in the literature.

TABLE II
R^2 VALUES FOR VARIOUS MODELS OF $\mu = f(F_n)$.

	$aF_n + b$	$1/(aF_n + b)$	$a/F_n^3 + b$
Paint Primer	0.56	0.59	0.29
Smooth Paper	0.48	0.51	0.24
Heavyweight Paper	0.43	0.44	0.24
Canvas	0.25	0.25	0.13

2) Additional Friction Parameters: In this work, we focused on the relationship between friction vs. normal force and contact velocity. When other sensing modes become available, this model can be easily expanded into a more complex multi-variable function by incorporating new parameters such as temperature, humidity, and contact area, whose relationship to μ is not constrained to a linear model.

D. Conclusion and Future Work

In conclusion, modeling friction as a stochastic function that varies with respect to normal force and contact velocity can better handle the complexities involved in frictional phenomena, which is key for advancing reliable grasping and manipulation. This can enhance a range of robotics applications, including analytical grasp modeling and planning, machine learning approaches, or physics engines for simulations. In future work, we aim to apply this model to more real-world grasping and manipulation planning and analysis on everyday objects with a more diverse set of surface materials, geometries, weight, texture, and stiffness.

ACKNOWLEDGMENT

REFERENCES

[1] R. Johansson and G. Westling, "Roles of glabrous skin receptors and sensorimotor memory in automatic control of precision grip when lifting rougher or more slippery objects." *Experimental brain research*, vol. 56, pp. 550–564, 1984.

[2] M. Mahdi, G. Ardakani, J. Bimbo, and D. Prattichizzo, "Quasi-static Analysis of Planar Sliding Using Friction Patches," *The International Journal of Robotics Research*, 2020.

[3] Q. Lu, A. B. Clark, M. Shen, and N. Rojas, "An Origami-Inspired Variable Friction Surface for Increasing the Dexterity of Robotic Grippers," *IEEE Robotics and Automation Letters*, vol. 5, no. 2, pp. 2538–2545, 2020.

[4] H. Khamis, B. Xia, and S. Redmond, "Real-time friction estimation for grip force control," in *IEEE International Conference on Robotics and Automation (ICRA)*, 2021.

[5] O. Khatib and B. Siciliano, *Springer handbook of robotics*. Springer International Publishing., 2016.

[6] S. Sills, K. Vorvolakos, M. K. Chaudhury, and R. M. Overney, "Molecular origins of elastomeric friction," *Fundamentals of friction and wear*, pp. 659–676, 2007.

[7] K. Viswanathan and S. Chandrasekar, "Fifty years of Schallamach waves: from rubber friction to nanoscale fracture," 9 2022.

[8] B. N. Persson, "On the theory of rubber friction," *Surface Science*, vol. 401, no. 3, pp. 445–454, 1998.

[9] B. Persson, "Theory of rubber friction and contact mechanics," *Journal of Chemical Physics*, vol. 115, no. 8, pp. 3840–3861, 8 2001.

[10] B. N. Persson, O. Albohr, U. Tartaglino, A. I. Volokitin, and E. Tosatti, "On the nature of surface roughness with application to contact mechanics, sealing, rubber friction and adhesion," 1 2005.

[11] A. Schallamach, "The Load Dependence of Rubber Friction," *Proceedings of the Physical Society, Section B*, vol. 65, 1952.

[12] P. Thirion, "Rev Gen Caoutch," vol. 23, 1945.

[13] A. Schallamach, "The Velocity and Temperature Dependence of Rubber Friction," Tech. Rep., 1953.

[14] G. Albertini, S. Karrer, M. D. Grigoriu, and D. S. Kammer, "Stochastic properties of static friction," *Journal of the Mechanics and Physics of Solids*, vol. 147, 2 2021.

[15] W. S. Kang, C. K. Choi, and H. H. Yoo, "Stochastic modeling of friction force and vibration analysis of a mechanical system using the model," *Journal of Mechanical Science and Technology*, vol. 29, no. 9, pp. 3645–3652, 9 2015.

[16] A. Bicchi, J. K. Salisbury, and D. L. Brock, "Experimental Evaluation of Friction Characteristics With an Articulated Robotic Hand." Toulouse, France: Springer Berlin Heidelberg, 6 1993.

[17] M. R. Cutkosky and P. K. Wright, "Friction, Stability and the Design of Robotic Fingers," *The International Journal of Robotics Research*, vol. 5, no. 4, pp. 20–37, 1986.

[18] H. Y. Han, A. Shimada, and S. Kawamura, "Analysis of friction on human fingers and design of artificial fingers," in *Proceedings - IEEE International Conference on Robotics and Automation*, vol. 4. IEEE, 1996, pp. 3061–3066.

[19] J. Zhou, J. A. Bagnell, and M. T. Mason, "A Fast Stochastic Contact Model for Planar Pushing and Grasping: Theory and Experimental Validation," 5 2017. [Online]. Available: http://arxiv.org/abs/1705.10664

[20] D. Ma and A. Rodriguez, "Friction Variability in Planar Pushing Data: Anisotropic Friction and Data-collection Bias," *IEEE Robotics and Automation Letters*, vol. 3, no. 4, pp. 3232–3239, 2 2018.

[21] J. K. Salisbury, "Interpretation of contact geometries from force measurements," in *IEEE International Conference on Robotics and Automation*, 1984, pp. 240–247.

[22] D. C. Montgomery and G. C. Runger, "Chapter 12: Multiple Linear Regression," in *Applied statistics and probability for engineers*. John Wiley & Sons, 2010, pp. 450–512.

[23] W. Chen, H. Khamis, I. Birznieks, N. F. Lepora, and S. J. Redmond, "Tactile Sensors for Friction Estimation and Incipient Slip Detection - Toward Dexterous Robotic Manipulation: A Review," *IEEE Sensors Journal*, vol. 18, no. 22, pp. 9049–9064, 11 2018.

[24] J. W. James and N. F. Lepora, "Slip detection for grasp stabilization with a multifingered tactile robot hand," *IEEE Transactions on Robotics*, vol. 37, no. 2, pp. 506–519, 4 2021.

[25] Y. Wang, X. Wu, D. Mei, L. Zhu, and J. Chen, "Flexible tactile sensor array for distributed tactile sensing and slip detection in robotic hand grasping," *Sensors and Actuators, A: Physical*, vol. 297, 10 2019.

[26] S. Teshigawara, T. Tsutsumi, S. Shimizu, Y. Suzuki, A. Ming, M. Ishikawa, and M. Shimojo, "Highly sensitive sensor for detection of initial slip and its application in a multi-fingered robot hand," in *Proceedings - IEEE International Conference on Robotics and Automation*, 2011, pp. 1097–1102.

[27] F. Veiga, J. Peters, and T. Hermans, "Grip Stabilization of Novel Objects Using Slip Prediction," *IEEE Transactions on Haptics*, vol. 11, no. 4, pp. 531–542, 10 2018.

[28] J. Bohg, A. Morales, T. Asfour, and D. Kragic, "Data-driven grasp synthesis-A survey," *IEEE Transactions on Robotics*, vol. 30, no. 2, pp. 289–309, 2014.

[29] H. Zhu and V. Kumar, "Dexterous Manipulation with Deep Reinforcement Learning:Efficient, General, and Low-Cost," in *International Conference on Robotics and Automation (ICRA)*, 2019.

[30] Z. Liu and R. D. Howe, "Overlooked Variables in Compliant Grasping and Manipulation," in *ICRA 2022 Workshop: Compliant Robot Manipulation: Challenges and New Opportunities*, 2022.

[31] ——, "Friction Variability and Sensing Capabilities for Data-Driven Slip Detection," in *IEEE/RSJ International Conference on Intelligent Robots and Systems (IROS) Workshop: The role of uncertainty and how it is tackled in robotic grasping and manipulation*, 2022.

[32] A. Koenig, Z. Liu, L. Janson, and R. Howe, "The Role of Tactile Sensing in Learning and Deploying Grasp Refinement Algorithms," in *IEEE/RSJ International Conference on Intelligent Robots and Systems (IROS)*, 2022.